Influence of Advection on Marine PBL Development

Ye Weizuo (叶维作)
Institute of Atmospheric Physics, Academia Sinica, Beijing 100029, China
Received April 19, 1990; revised September 25, 1990

ABSTRACT

Based on the DRS model (one coupled dynamical–radiational model of stratocumulus), though extended to take advection into account, several calculations have been made to estimate its contributions to the thermodynamical structure of the PBL (planetary boundary layer). Advection various calculations show does affect the development of the PBL, particularly in cloud forming and evolving. One of the intriguing findings which accords well with observations demonstrates that cold currents create strong convective weather, while warm currents bring about stable weather: produce prolonged low clouds or fogs.

I. INSTRUCTION

In two previous papers (Ye, 1990 and Ye, 1990; hereafter referred to as Ye1 and Ye2, respectively), the author established the DRS model to investigate the process of the development of marine boundary layers. The DRS model contains main physical mechanisms, such as large–scale vertical motions, eddy transfer, short– and long–wave radiations and precipitations; and all of these calculations are parameterized. Applications of the DRS model are discussed in Ye2, including the integration of the model to estimate some time constants, e.g., CFT (cloud forming time) and CLT (cloud life time). As indicated in Ye2, the DRS model is one–dimensional; the average quantities refer to an area over which changes due to the horizontal gradient are small, so the advective changes have been neglected. One of the main defects in ignoring advection is the fast approaching of the calculated air temperature $T(0)$ to the surface temperature T_s as the heat fluxes from the sea are the main cooling or heating source of the boundary layer before clouds form. In real thermodynamical surroundings, however, the air–sea temperature difference may persist very long owing to invasions of other weather systems, such as the contribution from advection. A typical example of this phenomenon is the case in which a cold front moves over a warmer water surface, or the opposite.

To overcome these flaws, as a sequel to Ye1 and Ye2, the author has in this study incorporated advection effects into the DRS model. In what follows it is assumed that a cold or warm air mass is passing over a sea or other water surface, but there is no difference in humidity between the current and local airs. Further, as the model is one–dimensional, the temperature gradient is set constant, which is reasonable for a short time, say several hours.

II. FORMULATIONS

It is proved (Schubert at al., 1979) that with advection contribution considered the mixed layer models are still able to be employed. There are a large number of equations defining the entrainment velocity, rainfall rate, as well as temperature and humidity distributions; please consult Ye1 and Ye2 if interested in details. We will next briefly derive only the temperature equation as it should be changed after the advective heating or cooling is added.

Based on the conservation of energy, present below is the equation for the equivalent potential temperature θ_e, a measure of the moist energy

$$\frac{\partial \theta_e}{\partial t} = -\frac{\partial \overline{w'\theta'_e}}{\partial z} - \frac{\partial R}{\partial z} - v\frac{\partial \theta_e}{\partial L} , \tag{1}$$

where $\overline{w'\theta'_e}$ is the heat flux; R, the radiation flux normalized by the density and specific heat C_p; v and L are the horizontal wind speed and the distance along the wind direction, respectively. As the name indicates, most mixed layer models make a premise (Ye 1): there is a well–mixed structure, or some semi–conservatives, such as θ_e, q_T (the specific total humidity) and v (including the wind direction), are height– independent within the boundary layer or so–called mixed layer through the turbulent mixing; that is

$$\frac{\partial \theta_e}{\partial z} = \frac{\partial q_T}{\partial z} = \frac{\partial v}{\partial z} = 0 . \tag{2}$$

Integrating (1) from 0 to z_T (the top of the mixed layer) and taking note of (2) yield

$$\frac{\partial \theta_e}{\partial t} = \frac{(\overline{w'\theta'_e})_0 - (\overline{w'\theta'_e})_{z_T} + R(0) - R(z_T)}{z_T} - v\frac{\partial \theta_e}{\partial L} . \tag{3}$$

Using boundary conditions the mixed–layer models usually adopt

$$(\overline{w'\theta'_e})_0 = c_T v(\theta_{es} - \theta_e) , \tag{4}$$

$$(\overline{w'\theta'_e})z_T = R(z_H) - R(z_T) - w_e(\theta_e(z_H) - \theta_e) , \tag{5}$$

we will obtain

$$\frac{\partial \theta_e}{\partial t} = \frac{c_T v(\theta_{es} - \theta_e) + R(0) - R(z_H) + w_e(\theta_e(z_H) - \theta_e)}{z_T} - v\frac{\partial \theta_e}{\partial L} , \tag{6}$$

where 0, Z_T and Z_H are, respectively, the height of the sea surface, the top of the boundary layer and the inversion layer lying atop of the boundary layer (see Fig. 1, Ye1); C_T is the drag coefficient, θ_{es} and θ_e are the equivalent potential temperatures at the surface and the boundary layer, and w_e, the entrainment velocity. The temperature equation will easily be derived from (6) in conjunction with moisture equation (see Eq. (3.14), Ye1). It is shown from (6) that the equilibrium state of the marine boundary layer is determined by the competition between radiative cooling, the entrainment of the warm and dry air from the inversion layer, the sensible heating or cooling from the sea and advective heating or cooling.

The estimation of the entrainment velocity is the vital link to mixed layer models (Nicholls, 1984). Present in Ye1 is a new scheme for calculating w_e; in the followings, we will show that the calculating scheme remains good for the model calculations with advections.

The entrainment velocity w_e is connected with buoyancy fluxes and their vertical distributions, as well as the capping inversion strength given by

$$\Delta\theta_v = \theta_v(z_H) - \theta_v(z_T) , \tag{7}$$

where θ_v is the virtual potential temperature.

The buoyancy flux at the height of z is expressed as

$$(\overline{w'\theta'_v})_z = \begin{cases} 0.6(\overline{w'\theta'_e})_z - \theta((\overline{w'q'_T})_z - (\widetilde{w_T q_l})_z), & \text{within cloud,} \\ (\overline{w'\theta'_e})_z - \left(\frac{L}{c_p} - 0.61\theta\right)((\overline{w'q'_T})_z - (\widetilde{w_T q_l})_z), & \text{below cloud} \end{cases} \tag{8}$$

where $\overline{w'q_T}$ and $\overline{w'\theta'_e}$ are the total moisture and the heat fluxes, respectively, $\widetilde{w_T q_l}$ is the rainfall rate, which has been parameterized in Ye1; and the other symbols have conventional notations. Obviously, among the above quantities, $\overline{w'\theta'_e}$ is the only item whose expression may be altered after advection is added.

To find the expression of $\overline{w'\theta'_e}$, we integrate (1) from 0 to z, also take notice of (2), and then have

$$z\frac{\partial\theta_e}{\partial t} = (\overline{w'\theta'_e})_0 - (\overline{w'\theta'_e})_z + R(0) - R(z) - zv\frac{\partial\theta_e}{\partial L} \ . \tag{9}$$

Substituting (3) into (9) and rearranging it will present the expression for the heat flux as

$$(\overline{w'\theta'_e})_z = (\overline{w'\theta'_e})_0 + R(0) - R(z) - \frac{z}{z_T}((\overline{w'\theta'_e})_0 - (\overline{w'\theta'_e})_{z_T} + R(0) - R(z_T)) \ , \tag{10}$$

in which the advective items have been cancelled.

Equation (10) is formally the same as that without advection (see Eq. (3.5), Ye1). This is physically caused by above–mentioned θ_e and v being z–independent; i.e., due to the turbulent mixing, advection influences the heat flux implicitly through the change in the heat flux at the surface. This can be shown from (3), (4), and (10). Consequently, the scheme for the entrainment velocity will be identical to that in Ye1 where no advection is involved.

As in Ye2, a paper dealing with applications of the DRS model, the MLS (Midlatitudinal Summer Atmosphere, McClachy et al., 1972) profile with a large–scale subsidence is adopted for the initial thermodynamical structures of the atmosphere except that to investigate a wider range of situations, three temperature profiles under 2 km where the PBL is usually located are used: the thermal profile remains the same as in the MLS above 2 km., but diverges to three branches below 2 km; in particular, $T(0,0)$ and $T(2\text{km}, 0)$ are equal to, respectively, 293 and 284 K, 294 and 285 K, and 295 and 286 K. In addition, 5 m / s of the surface wind and 0.01 K / Km of a horizontal temperature gradient are postulated, and hence the advective temperature change rate would be ± 4.2 K / day, a value close to the radiative cooling rate at the surface and representative of the maritime climate (Schubert, 1979). Finally, following Ye 2 10 and 30 minutes of a time–step are selected for clear and cloudy skies, respectively.

III. RESULTS AND ANALYSES

By time–marching (integration) the model has been run from 17:00 with an initial boundary layer of 100 m till 32:00 or anytime when produced Sc breaks up. Time–series results (with and without advection) are given of the surface air temperature $T(0)$, the entrainment velocity w_e and the height of the boundary layer top Z_T in Tables 1, 2 and 3 for different initial surface air temperatures $T(0,0)$, where n–case, w–case and c–case,

respectively, stand for the case of no advection and those with warm and cold advections.

Table 1. Time series of the PBL thermodynamical structure with $T_s = 294$ K and $T(0,0) = 295$ K, where z_T is the top of the PBL and also the top of the Sc after it occurs, Z_b is the Sc base

Time		$T(0)$ K	w_e (cm / s)	Z_b (m)	Z_T (m)
17:00	C	295	0		100
	N	295	0		100
	W	295	0		100
18:00	C	294.45	0		99.4
	N	294.61	0		99.4
	W	294.77	0		99.4
19:00	C	294.04	0.25		99.6
	N	294.32	0		98.9
	W	294.60	0		98.9
20:00	C	293.80	1.14		117.2
	N	294.11	0.14		98.7
	W	294.47	0		98.3
22:00	C	293.56	0.81		184.6
	N	293.97	0.51		131.2
	W	294.30	0		97.3
24:40	C	293.21	1.21	262.5	267.7
	N	293.80	0.42	–	171.2
	W	294.24	0	93.9	95.8

Table 1 shows cold water cases where $T(0,0)$ is one degree higher than the sea temperature T_s, which Ye2 indicates belongs to stable boundary layers. At the beginning, as explained in Ye2, the boundary layers cannot develop ($w_e = 0$), so they shrink because of the large–scale subsidence. One hour later (18:00), all three boundary layers (n–, w– and c–cases) cool down, although in different degrees due to advection effects. The cooling results from radiation and the sensible heat transfer down to the sea; the latter is dominant at the beginning when the PBL is thin and the air–sea temperature difference is large. For c–case the main physical processes, radiation, sensible heat transfer and advection all decrease the temperature of the PBL, and hence the $T(0)$ there is the lowest compared with those in n– or w–case. At 19:00, although the $T(0)$ of c–case is still a bit greater than T_s ($T(0)$ and T_s are θ and θ_s for the sea level, then the sensible heat flux $(\overline{w'\theta'})_0 = c_T v(\theta_s - \theta)$ is negative), the c–case boundary layer starts growth. This can be briefly explained as follows: the buoyancy flux from the sea, by definition, is expressed as

$$(\overline{w'\theta'_v}) = c_T v(\theta_{vs} - \theta_v) \tag{11}$$

$$\theta_{vs} = \theta_s(1 + 0.61 q_s) \tag{12}$$

$$\theta_v = \theta(1 + 0.61 q) \ . \tag{13}$$

As the saturation humidity at the sea surface q_s is much higher than the humidity in the boundary layer q, present in (13) is a (though small) positive buoyancy flux, which is the main source of eddy before cloud forms (Ye 1). Then follows the PBL of n–case at 20:00, while the PBL of w–case still shrinks as its temperature $T(0)$ remains much higher than T_s owing to the warm advection.

Table 2. Same as Table 1, except $T(0,0) = 293$K

Time		$T(0)$ (K)	w_e (cm / s)	Z_B (m)	Z_T (m)
17:00	C	293	0.92		100
	N	293	0.92		100
	W	293	0.92		100
18:00	C	293.21	2.55		170
	N	293.37	2.25		167
	W	293.53	1.94		164
20:00	C	293.09	1.40		301
	N	293.51	0.96		275
	W	293.91	0.56		248
21:00	C	292.98	1.25		349(CFH)
	N	293.51	0.89		308
	W	294.04	0.35		264
21:30	C	292.87	3.52	350.2	377
	N	293.50	0.82	–	323
	W	294.04	0.28	–	270

Warm–sea cases are calculated and compared in Table 2, where the initial air temperature $T(0,0)$ is one degree lower than T_s. As fully discussed in Ye 2, warmer sea brings about an unstable development of the PBL in which the entrainment velocity is usually very high. This is also verified in Table 2, from which it can be seen that the three simulated boundary layers grow quickly even before the clouds take place. Nevertheless, advections also affect the rates of the PBL growth. The PBL temperature differences due to different advections among $n-$, $w-$ and c–cases lead to variations of the air–sea temperature difference, which Eqs. (11)–(13) show connects directly to the buoyancy flux. Specifically, the cold advection offsets the sensible heating from the sea, restricts the quick increase of $T(0)$, maintains strong buoyancy flux from the sea and the vigorous PBL development results. Conversely, for w–case the additional heating from the advection to the sensible heating coming from the sea impels the increase of $T(0)$, efficiently reduces the buoyancy flux from the sea, and hence stunts the PBL advancing. The thermodynamical conditions of n–case, as expected, lie between those of $c-$ and w–cases; before 21:00 (the time the c–case cloud forms) its entrainment velocity, PBL height z_T and air temperature $T(0)$ are almost the mean of corresponding values of $c-$ and w–cases.

The results of $T(0,0) = 294$ K for three advection cases are listed in Table 3. It is clear that due to the closeness of air and sea temperatures at the beginning, there is little sensible heat from the sea, and therefore advections make dominant contributions to the cooling or heating in the three simulated PBLs. As time goes on, the air temperatures $T(0)$ of w–case and c–case, respectively, make plus and minus departures from T_s, and their entrainment velocities show corresponding variations; the w_e in c–case is much greater than the w_e of w–case. At 23:00, 6 hours later from the beginning, the PBL of c–case reaches 314 m high, 2.5 times that of w–case.

For clearer representation of the whole process of the PBL development, the above described time evolutions of PBLs are plotted in Figs 1, 2 and 3, in which N, W, C stand, as before, for with no, warm and cold advections, respectively; +1, 1, −1, stand, respectively, for $T(0.0) = 295$, 294, and 293 K, and cloud range, if any, is also enclosed.

Table 3. Same as Table 1, except $T(0,0) = 294K$

Time		$T(0)$ (K)	w_e (cm / s)	Z_B (m)	Z_T (m)
17:00	C	294	0.24		100
	N	294	0.24		100
	W	294	0.24		100
18:30	C	293.75	1.59		132
	N	293.95	1.06		124
	W	294.16	0.48		116
20:00	C	293.55	1.03		202
	N	293.91	0.67		173
	W	294.22	0.17		138
21:30	C	293.35	1.16		241
	N	293.83	0.65		204
	W	294.21	0		139
23:10	C	293.07	1.72	314	320
	N	293.76	0.61	–	239
	W	294.19	0	–	138

First, looking at Fig 1, it is mere coincident that clouds form at the same time (24:30) for both c– and w–cases, as the causes of their cloud forming are quite different. For c–case, as indicated before, the cold advection reduces the air temperature, assists the upwelling buoyancy from the sea; and the PBL advances quickly. Once the humidity of the top of the PBL approaches the saturation humidity there, cloud forms. As a non–convective Sc case, cloud forming in w–case, however, physically differs: there are steady fluxes of the abundant vapor from the sea and no upper dry air coming down from the inversion layer due to the entrainment velocity $w_e = 0$, so the air there becomes fast moistened and stratum cloud forms accordingly. If the condensation occurs near the surface, fogs will take place (McBean, 1985). As for n–case, there is neither the c–case PBL quickly jumping–induced temperature decrease at the top of the PBL, nor the violent moistening in w–case; these two factors hold back n–case cloud forming until 27:30, when clouds for both c– and w–cases have already dissipated (it will be mentioned again later).

In addition, the inspection of each figure reveals that the CFT (cloud forming time), the time period from the beginning when the model is run (17:00, at the present calculations) to the time when the simulated cloud forms) and the CFH (cloud forming height) are also affected by advection; the cold advection promotes PBL development, shortens CFT and heighten CFH, while the warm advection shows the opposite behaviors.

Then, cross–referring the three figures, we can easily find that developments of boundary layers vary widely with their initial temperatures $T(0,0)$; with the same advection, the lower $T(0,0)$ is, the quicker the PBL grows. As mentioned before, there are two main types of Sc–forming mechanisms: non–convective (e.g., curves $W+1$ and $W0$ (before 27:30)) and convective (e.g., the rest of cases). For convective cases, with an identical advection heating or cooling, CFT decreases and CFH increases with the decrease of $T(0,0)$; i.e., the cooler the initial air is, the faster and at higher position cloud will produce. To boot, it can further be illustrated that with the same $T(0,0)$, the convective Sc will mostly form quicker and reach higher than non–convective Sc does.

Lastly, turning to cloud life time (CLT), two features can be identified through comparisons. First, the air–sea temperature difference plays an important role in CLT; cooler sea ($T_s < T(0,0)$) stabilizes the PBL and prolongs the CLT, while warmer sea ($T_s > T(0,0)$) drives the eddy, promotes the convection, assists the break–up of the cloud, and accordingly shortens the CLT. This relation between CLT and the difference between air and sea temperatures is in detail demonstrated and proved in Ye2. Comparison of the three curves in every figure also suggests the influences of advections on CLT: the cold advection, as mentioned above, reduces the air temperature, decreases the air–sea temperature difference, and gains cloud maintenance; whereas the warm advection shows the opposite effects. This feature is mostly representatively reflected in Fig.3, where CLTs for *c*–, *n*– and *w*–cases are, respectively, 1.5, 3 and > 8 hours. One exception is the case of $W+1$, where the advective cooling can not lengthen the CLT. In fact, $W+1$, as previously described, belongs to a non–convective case in which the PBL becomes strongly moistented by upwelling moisture flux from the sea and shrinks owing to the large–scale subsidence. Once the cloud exists, its top–radiative cooling creates a powerful eddy source (Nicholl, 1984), and then, when this eddy energy is greater than the sensible heat loses downward to the sea, the PBL will develop (see Curve W0), On the other hand, the moistening of the PBL makes much greater the humidity difference between the PBL and the air above. The virtual potential temperature defined in (12) is a measure of the buoyancy. Therefore, the fast humidity increase in the PBL makes possible buoyancy decrease across the inversion layer (i.e., $\Delta\theta_v < 0$ see (7), although temperature still increases upward (i.e., $\Delta\theta > 0$). Normally, the inversion layer acts for a restraint of the PBL development, or makes it grow stably (Nicholl, 1984). With a negative $\Delta\theta_v$, the inversion layer becomes another eddy source instead of a sink, and the PBL will run away and the cloud breaks up quickly (Deardorff, 1980). It should be noted, however, that in the present calculations, as assumed at the beginning of the paper, only horizontal temperature variations are considered. If the advectional changes in humidity are also involved, it is believed that the above–mentioned "moisture heap" in one area will vanish or diminish. Accordingly, it follows from these analyses that the above–mentioned exception in $W+1$ to the rule that cold advection prolongs CLT results just from the negligence of moisture advection transfer. Finaly it is worthy of being pointed out that the results in this section would make quantitative but not qualitative changes when there is a variation of ± 3 K / day in the advective temperature change rate.

Jemes and Lenschow (communications, 1988), who have been studying and observing the PBL clouds for many years, indicated that there are different kinds of clouds off California in summer and in winter. In summer, when warm air passes over colder water, there exist persistent low clouds or fogs (if wind is very weak); in winter when very cold air moves from the North American Continent over warmer water, strongly convective Sc or cumulus often develops but lasts a very short time. Also, Agee (1985) and Randall (1985) had similar conclusions. Admittedly, their observations and comments provide strong verifications of our model's results concerning CLT versus advection.

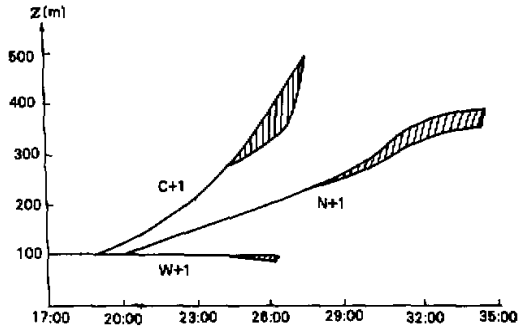

Fig.1. Time-dependent PBL with $T_s = 294$ K and $T(0,0) = 295$ K, where the hatched areas indicate the clouds.

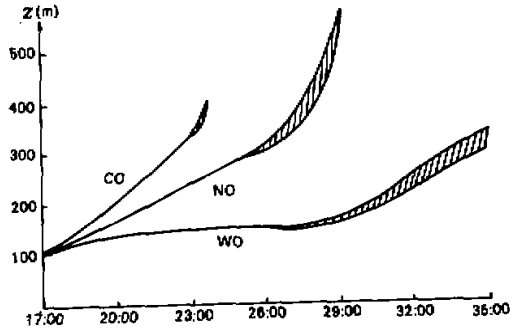

Fig.2. Time-dependent PBL with $T_s = 294$ K and $T(0,0) = 294$ K, where the hatched areas indicate the clouds.

IV. CONCLUSIONS AND SUMMARY

In anticipation of the advent of cold or hot waves, the DRS model has been expanded in which terms of advective cooling or heating rates are added. Through the expanded DRS model, several calculations have been made, and the following conclusions can be reached as a summary. Advective cooling or heating, although mere ± 4.3 k/day in present calculations, would effectively affect the PBL development: cold advection cools the air,

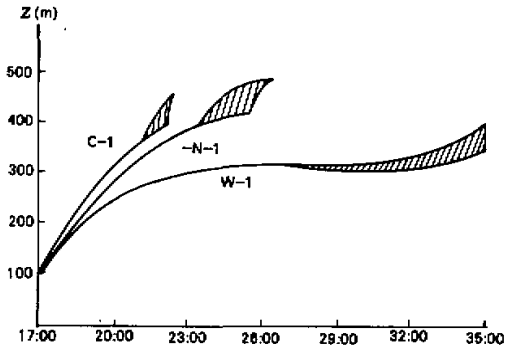

Fig.3. Time–dependent PBL with $T_s = 294$ K and $T(0,0) = 293$ K, where the hatched areas indicate the clouds.

drives the buoyancy flux from the water and hence promotes the PBL growth; while warm advection stifles it. Furthermore, with otherwise equal conditions, if cold advection is taken into account, Sc takes place earlier and higher than that without advection, and even more than that with warm advection, except when the PBL shrinks and non–convective Sc or fog occurs. Finally, as the temperature change made by advection readjusts the air–sea temperature difference, which has strong influence on CLT, advection also contributes to CLT: warm advection increases the air temperature, stabilizes the boundary layer, and consequently prolongs Sc; conversely cold advection stirs up the growth of the boundary layer, causes unstable weathers, and therefore, Sc, even once formed, can hardly maintain—all these features have been tested against observations.

REFERENCES

Deardorff, J. W. (1980), Stratocumulus–capped mixed layer derived from a three–dimensional model. *Boundary–layer Meteor.*, **18**: 495–521.

Agee, Ernest M. (1985), Extratropical Cloud–topped boundary layers over the oceans. WMO, Appendix B.

McBean Gordon. (1985), The cloud–topped boundary layer. WMO, Appendix c.

Nicholls, S. (1984), The dynamics of stratocumulus: Aircraft observations and comparisons with a mixed layer model, *Quart. J. Roy. meteor. Soc.* **112**: 461–480.

Randall, David A. (1985), Key problems of parameterizations for simple cloud–topped boundary layer model. WMO, Appendix J.

WMO, (1985), Report of the JSC / CAS workshop on modelling of cloud topped boundary layer. World Climate Research Programme, WMO / TD. NO. 75, World Meteorological Organization, Geneva. Switzerland.

Schubert, Wayne H., Joseph S. Wakefield, Ellen J. Steiner and Stephen K. Cox.(1979), Marine stratocumulus convection, Part II Horizontally inhomogeneous solutions. *J. Atmos. sci.*, **36**: 1308–1324.

Ye, Weizuo. (1990), A coupled dynamical–radiational model of stratocumulus, *Advances in Atmospheric Sciences*, **2**: 197–210.

Ye Weizuo. (1990), Application of the coupled dynamical–radiational model of stratocumulus, *Advances in Atmospheric Sciences*, **3**: 331–346.